# Green Chemistry

## ARTICLE

# Utilization of softwood lignin as both crosslinker and reinforcing agent in silicone elastomers

Jianfeng Zhang,[a] Yang Chen,[a] Paul Sewell[a] and Michael. A. Brook,*[a]

Lignin, the second most abundant naturally occurring organic polymer on earth, is normally used only as a source of fuel because of the difficulties in processing it for other applications. While the Piers-Rubinsztajn reaction of phenols and alkoxybenzene groups with hydrosilanes can lead to highly degraded hardwood lignin, under different conditions, the process permits partial reduction of surface-presenting groups on softwood lignin. The method requires no pre-modification of the lignin surface, which reacts with silcon-hydride functional groups on silicone polymers in a process catalysed by $B(C_6F_5)_3$. Simultaneously, crosslinking of the silicone occurs to give a reinforced elastomer. Lignin plays dual roles as crosslinker and reinforcing reagent. The mechanical performance of lignin crosslinked/reinforced composites, depending on formulation, is comparable to some commercially available silicone elastomers and can be readily tuned by lignin content and molecular weight of silicones used in the formulation. The composites demonstrated acceptable resistance to solvent extraction and excellent resistance to high temperature aging.

## Introduction

Lignin is one of the most abundant naturally occurring polymers on the earth. However, the majority of lignin that is recovered, typically from kraft pulping processes, is burned as a low value fuel. In one important exception, lignin emerged as a "green" renewable source for vanillin in early 1940s.[1] In recent decades, several methods have been developed with the aim to convert lignin into value-added products, including biodegradation, thermochemical depolymerization, and catalytic valorization.[2-4] However, few successes on depolymerizing actual lignin into monomeric molecules have been achieved with a high conversion yields.[5-8]

The low efficiency of lignin depolymerization process is due to its complex structure and the types of linkages present.[3] The building units and polymeric network architecture of lignin vary depending on the species.[9] Typically, the lignin derived from grass and softwood contains more guaiacylpropane (G) units; hardwood lignin consists of approximately equal proportinos of guaiacylpropane (G) and syringylpropane (S) units.[10] These units are mostly bridged by β-O-4 linkages;[11] complemented with other linkages such as 5-5, β-5, 4-O-5, β-1, and β-β, known for resistance to chemical degradation (Scheme 1).[3, 10, 12]
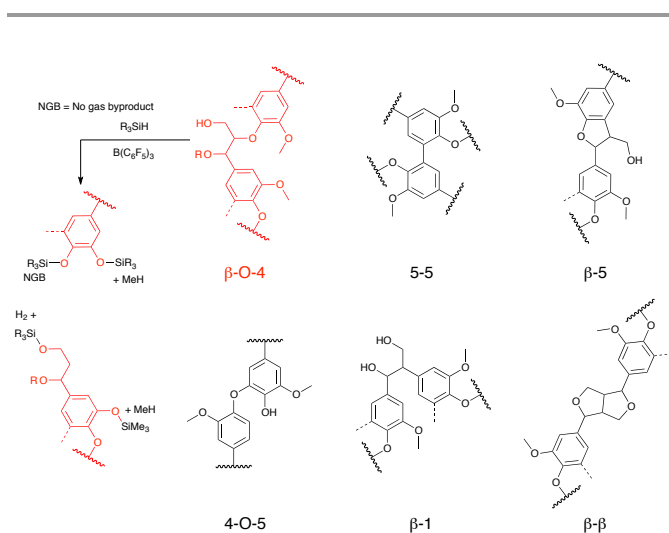


Scheme 1. The typical linkages in lignin molecules that are backbone cleavable (red) and partly degradable (black) under Piers Rubinsztajn conditions.

An alternative strategy to utilize lignin for industrial applications would take advantage of its inherent strength.[13] Lignin has been examined as a filler/crosslinker in a variety of resins, including phenolic,[14, 15] epoxy,[13, 16-18] polylactide,[19, 20] and polyurethane resins.[21-23] The hydroxyl groups found on lignin are readily ester functionalized with succinic anhydride leaving residual carboxylic acids that were used as a curing agent for epoxy resins.[13] The epoxy resin had excellent properties with a high lignin content (up to 32.3%).[13, 18] In a

separate report, polyurethane (PU) prepared from a hydroxy rich lignin in which methoxy groups had been hydrolyzed demonstrated enhanced mechanical properties compared to the unmodified lignin-base PU.[21] More recently, softwood lignin was used as a multifunctional phenolic component to synthesize poly(arylene ether) sulfones.[24] These achievements demonstrate a promising application of lignin, as a phenolic precursor, for polymeric materials.

Although $B(C_6F_5)_3$ (tris(pentafluorophenyl)borane) facilitates reduction by hydrosilanes of functional groups, including alcohols, aldehydes, ketones, carboxylic acids, esters, phenol, and alkoxyphenyl, in presence of silicon hydride,[25-31] it was only recently exploited for the reduction/modification of lignin.[32, 33] In the presence of hydrosilanes, $B(C_6F_5)_3$ leads to cleavage of β-O-4 and α-O-4 linkages: silylation of phenols, methoxyl groups, and certain secondary alcohols occurs concomitantly under mild conditions (Scheme 1).

Silicone elastomers are used for applications ranging from biomaterials to microcontact printing.[34, 35] The poor tear resistance of silicones requires the use of filler reinforcements in order to achieve useful performance.[36] Minerals, particularly silica, are commonly used to reinforce silicone elastomer: reinforcement efficiency depends on loading, filler particle size and chemical nature of filler surface.[36, 37] Normally, high surface area fumed silica (nominal particle size ~10nm, aggregate size ~ 50 nm) is prepared by burning $SiCl_4$. As much as 30% or more silica may be included in a silicone elastomer formulation.

Silicone elastomer networks are prepared using the Piers-Rubinsztajn reaction by crosslinking hydrosilicones with alkoxysilanes in the presence of fillers (Scheme 2A). Instead of using tetraethyl orthosilicate (TEOS) as a crosslinker,[38, 39] we reasoned that is could be possible to obtain reinforced silicone elastomers from the reaction of hydrogen-terminated polydimethylsiloxane (H-PDMS-H) with softwood lignin, catalyzed by $B(C_6F_5)_3$) (Scheme 2B). The controlled generation of silicone elastomers formed with the less dense, biodegradable, renewable filler softwood lignin is reported below.

## Experimental Section

### Materials

Hydride functional silicone: pentamethyldisiloxane (PMDS), hydride-terminated PDMS (DMS-H11, H21, H31, and H41, with molecular weights for 1175, 6000, 28000, and 62700 g/mol, respectively), poly(hydromethylsiloxane) (PHMS, Mw = 1800-2100 g/mol), and poly(hydromethyl-siloxane)-poly(dimethylsiloxane) (PHMS-PDMS) copolymer (HMS-301, Mw = 1900 ~ 2000 g/mol, and HMS-501, Mw = 900 ~ 1200 g/mol) were purchased from Gelest (Table 2). $B(C_6F_5)_3$ (BCF) was purchased from Sigma-Aldrich, and stored as a stock solution (40 mg/ml, 78.13 mM) in dry toluene. With the exception of decamethylcyclopentasiloxane ($D_5$, ($Me_2SiO)_5$, Gelest), solvents were purchased from Caledon

Laboratories and used after drying over activated alumina. Antifoam 2210 was used as received from Dow Corning.
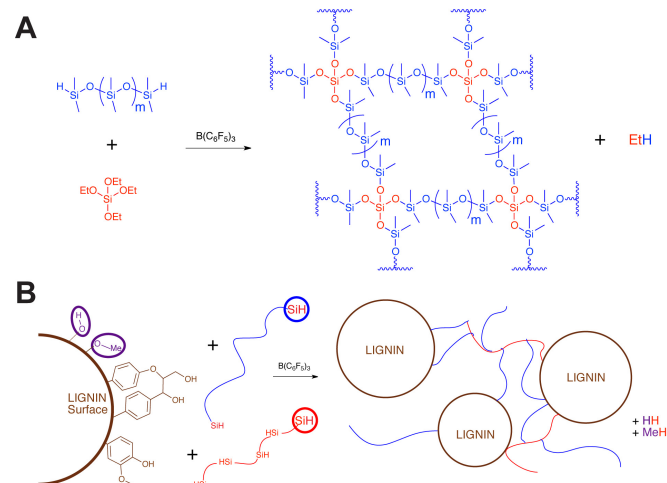


Scheme 2. Reaction scheme: A: Piers-Rubinsztajn process for elastomer formation; B: Replacement of alkoxysilane by lignin for both crosslinking and physical reinforcement.

Softwood kraft lignin (SKL) was provided by Weyerhaeuser (denoted as SKL-W) or purchased from Sigma-Aldrich (SKL-S). Prior to use, the lignin samples were milled into smaller particles sizes (~3 g portion of lignin and 10 steel balls with diameter of 3 mm were placed in a 25 ml PE container; a Flacktek speed mixer served as the ball-mill at a speed of 3500 rpm). The lignin powder was pass through a 75 μm sieve: oversized particles were discarded. The SKLs were stored, with drying, in a desiccator under vacuum and over Dri-rite. Although we examined two different sources of lignin, there were no significant differences in elastomer properties as a function of SKL origin.

### Quantitation of reactive surface functional groups on lignin particles

The concentration of lignin surface functional groups (hydroxyl, methoxyl, β-O-4 and α-O-4) was determined by measuring the volume of gaseous by-products (methane, $H_2$, etc.) formed during the reaction with hydrosilicones. The generated gas was collected by a water displacement method (ESI †). Several different hydride functional silicones were used in these experiments, but a common procedure was used with each of them. Lignin powder (ranging from 5 to 200 mg) was dispersed in dry toluene (3 ml) to which was added $B(C_6F_5)_3$ (10 μL in toluene, 40mg/ml, 0.8 μmol) with stirring. After sealing the vessel with a septum, a portion of hydride functional silicone (PMDS, DMS-H11, HMS-301, 501, or 992, 1 ml) was injected. The suspension was allowed to stir until no further volume changes were observed in the burette (which took from 2 - 8 h). When the reaction was complete, the modified lignin was washed with dry toluene (10 ml x 6 times, followed by centrifugation using a Thermo Durafuge 100 at 4000 rpm for 20 min after each wash cycle) to remove adsorbed (i.e., not covalently bonded) silicone from the lignin. Finally,

the lignin was dried at 70 °C under a nitrogen blanket, then characterized using IR diffuse reflectance infrared in Fourier transform mode (DRIFTS, Thermo Nicolet 6700).

Table 1. Use of lignin as crosslinker/reinforcement in silicone elastomers

| Lignin elastomer* | Lignin % | Lignin mg | Hydride-terminated PDMS (mg) | HMS-992 (mg) | $D_5$ (ml) | $B(C_6F_5)_3$ (ppm) |
|---|---|---|---|---|---|---|
| LE-0.5 | 0.5 | 5 | | 21 | 0 | 273 |
| LE-05 | 5 | 50 | | 41 | 0 | 293 |
| LE-09 | 9 | 100 | | 50 | 0 | 278 |
| LE-16 | 16 | 200 | | 83 | 0.5 | 312 |
| LE-27 | 27 | 400 | | 102 | 0.8 | 319 |
| LE-41A | | | | 38.5 | | 326 |
| LE-41B | ~ 41 | 800 | | 154 | 1 | 307 |
| LE-41C | | | DMS-H31 | 308 | | 285 |
| LE-46 | 46 | 1000 | (1000) | 165 | 1.5 | 277 |
| LE-50 | 50 | 1200 | | 202 | 1.5 | 300 |
| LE-57 | 57 | 1600 | | 221 | 2 | 284 |
| LE-66 | 66 | 2400 | | 250 | 2 | 274 |
| LE-68 | 68 | 2800 | | 298 | 2.5 | 293 |
| LE-71 | 71 | 3200 | | 310 | 2.5 | 266 |
| | | | | | | |
| LE-41D | | | DMS-H21 (1000) | 38.5 | 0 | 326 |
| LE-41E | 41 | 800 | DMS-H11 (250) H21 (550) H31 (200) | 38.5 | 0 | 326 |
| LE-41F | | | DMS-H41 (1000) | 38.5 | 2 | 326 |
| LE-41G | 41 | 800 | DMS-H31 (842) | HMS-501 (312) | 1 | 307 |
| LE-41H | 41 | 800 | DMS-H31 (530) | HMS-301 (623) | 1 | 307 |

*Nomenclature: the number at the end of the label refers to the wt% lignin in the formula.

### Control Experiments

Control experiments were performed to examine the ability of unmodified lignin to reinforce silicone elastomers. Softwood lignin was therefore incorporated into both commercial Pt- and tin-catalyzed silicone elastomer formulations. For the Pt-catalyzed formulation, the vinyl-terminated PDMS (2g, DMS-V35:    $(CH_2=CH)Si(CH_3)_2O[Si(CH_3)_2]_nOSi(CH_3)_2(CH_2=CH)$, Mw = 28,000 g/mol, Gelest), PHMS (0.02 g, HMS-992), and lignin (1.5 g to give ~ 40% of lignin in elastomer) were hand mixed to give a homogeneous dispersion, then the platinum catalyst (~ 500 μl of xylenes solution containing 0.5% Pt, ~ 5000 ppm, diluted from Karstedt's catalyst stock solution purchased from Sigma-Aldrich) was added and immediately mixed with the suspension. Finally, the mixture was poured into a Petri dish and allowed to cure at 90 °C.

For the tin catalyst formulation, silanol-terminated PDMS (2g, DMS-S31, HO-Si(CH$_3$)$_2$O[Si(CH$_3$)$_2$]$_n$OSi(CH$_3$)$_2$-OH, Mw = 26,000 g/mol, Gelest), TEOS (0.08 g, tetraethyl orthosilicate, Sigma-Aldrich), and lignin (0.5 g for ~ 20% wt, 1.4 g for ~

40%, and 3.1 g for ~ 60% of lignin in elastomer) were hand mixed to give a homogeneous dispersion, then, the tin-catalyst (~ 50μl, dibutyltin dilaurate, 95%, Sigma-Aldrich) was mixed and poured into a Petri dish to curing at room temperature.

### Fabrication of lignin crosslinked/reinforced silicone elastomers

Lignin could be used directly as both a chemical crosslinking and reinforcing reagent for silicone elastomers (Table 1). As an example, a 200 mg portion of lignin was weighed and mixed with 1 g of hydrogen-terminated PDMS (e.g., DMS-H31). Depending on the percentage of lignin and molecular weight of hydride-terminated PDMS in the formula, a solvent (typically $D_5$ ~ 1 ml per 3.5 g formulation) was required to lower the viscosity. Thus, after hand mixing lignin, hydrogen-terminated PDMS and solvent into a homogeneous dispersion, Antifoam 2210 (1wt% with respect to the weight of elastomer precursor to reduce viscosity building), $B(C_6F_5)_3$ solution, and HMS-992 (acting as co-crosslinker) were added sequentially and mixed immediately. The formula was degassed at vacuum oven (685 mm Hg vacuum, VWR 1415M) at 40 °C for 12 h followed by a post-curing at 90 °C for another 12 h under the same vacuum. The formulation for elastomers with different lignin content and mechanical properties are list in Table 1.

### Characterization

Infrared spectroscopy was used to characterize the degree of functionalization of Si-H on lignin surface using diffuse reflectance infrared Fourier transform mode (DRIFTS, Thermo Nicolet 6700), as well as the surface of cured elastomers with attenuated total reflectance (ATR-IR). Shore A (MFG. Co. Inc., U.S. Patent 2453042) and Shore OO durometers (Rex Gauge Company, Inc. U.S. Patent 2421449) were used to characterize the hardnesses of the elastomers. The modulus and elongation-at-break of lignin/silicone elastomer were determined by a Universal Test System (INSTRON 3366, 50 N load cell). Both ends of the elastomer, cut into dumbbell shape, were clamped with grips, and then stretched using a crosshead speed of 20 mm/min. The dimensions (thickness and width) of tested elastomer specimens were measured with an electronic digital micrometer (Mitutoyo, Japan; 0.001-mm sensitivity) at three random positions. Thermogravimetric analysis (TGA, TA instruments Q50) was performed under air; the temperature range was set from 50 °C to 800 °C with a 10 degrees/min step. The lignin distribution within the elastomer was characterized using a microscope under TV mode (Zeiss, LSCM 510).

## Results and Discussion

The presence of lignin in traditional silicone elastomer formulations led to undesirable outcomes. No elastomer could be obtained from Pt-catalyzed formulation, even when a very large excess of catalyst (5000 ppm) was included. It is inferred that the functional groups found on SKL can act as ligands and poison the Pt-catalyst.[40] Although it was possible to make 20 to 60wt% lignin filled elastomers using tin-catalyzed room

temperature vulcanization, the product elastomers were very brittle and inflexible, showing very low elongation-at-break ratios.

Elastomers can be made using the Piers-Rubinsztajn reaction by combining alkoxysilanes with hydrogen-terminated silicones in the presence of $B(C_6F_5)_3$ (Scheme 2A).[38, 39] In such a case the stoichiometric ratio of functional groups SiH/SiOR is known from the specific chemical structures of the precursors. When considering the use of the ArOR groups in lignin as a crosslinking centre, however, the calculation is more complex. As a natural polymer with complex and random chemical structures, the functionality of lignin will vary from species to species and from sample to sample.[9] As the lignin will preferentially react at the particle surface, the number of available surface functional groups (hydroxyl, methoxyl, and β-O-4) will also be affected by factors including particle diameter, surface roughness, and aggregation, etc. Therefore, before using the lignin as a crosslinker, it was necessary to establish the concentration of reactive surface functional groups on lignin particles.

One equivalent of hydrogen/methane gas is formed from the silylation of a hydroxyl or methoxyl group, respectively, by $HSiR_3$. By contrast, the cleavage of an ether or silylether yields no hydrogen (or alkane) gas (Scheme 1).[27, 31] Therefore, it is possible to establish approximate concentrations of surface OH, OR, ethers and silyl ethers by titrating the surfaces of a known weight lignin particles with silicones containing a known concentration of SiH groups and measuring the gas produced (ESI †). As shown in Fig. 1, gas production (from HMS-501 for this model study) depended on the total amount of dispersed lignin.

In a homogenous solution, that is, if SKL was dissolved rather than dispersed, gas production should increase linearly with lignin content. However, it instead followed a power law in this heterogeneous dispersion because of changes in effective surface area over time. The aggregation of lignin particles occurs during the reaction to form aggregates of morphologies that are concentration dependent. The availability of surface functional groups depends on the nature of the aggregate (Fig. 1). As a consequence, the ratio of active surface area to mass dropped at increased lignin concentrations. At a low solid/liquid ratio, lignin particles were uniformly dispersed (5 mg/g, Fig. 1A), but formed clusters that gelled at higher solid/liquid ratios (50 mg/g → 200 mg/g). The concentration of reactive surface functional groups on the lignin surfaces was 0.8-11 μmol mg$^{-1}$ (Fig. 1).

These conclusions were supported by DRIFT-IR measurements. The intensity of the Si-H signal on lignin surfaces was found to decrease exponentially with lignin content in the solvent (ESI †). This finding was key to designing formulations for lignin-in-silicone elastomers with different lignin contents: the morphologies of lignin in the silicone, and the resulting elastomeric physical properties depended on surface area, functional group concentrations and amount of fluid present during preparation.

The network structure of the elastomer depends on the lignin as noted above, and also on the nature of the hydrido-silicones. As shown in Table 2, several different silicone hydrides, including mono-functional silicone (PMDS), di-functional silicone (DMS-H11), and multi-functional copolymer/polymers (HMS-301, 501, and 992) were doped with lignin. All of the silicone polymers tested reacted efficiently with lignin. The gas production exhibited no significant differences between the silicone hydrides tested (normalized to the same SiH/lignin ratio), and ranged about 4.9 to 5.8 ml (Table 2). Thus, the reactivities between lignin surface functional groups and silicone hydrides of different chemical structure are approximately the same under these conditions provided that the surface remains accessible.
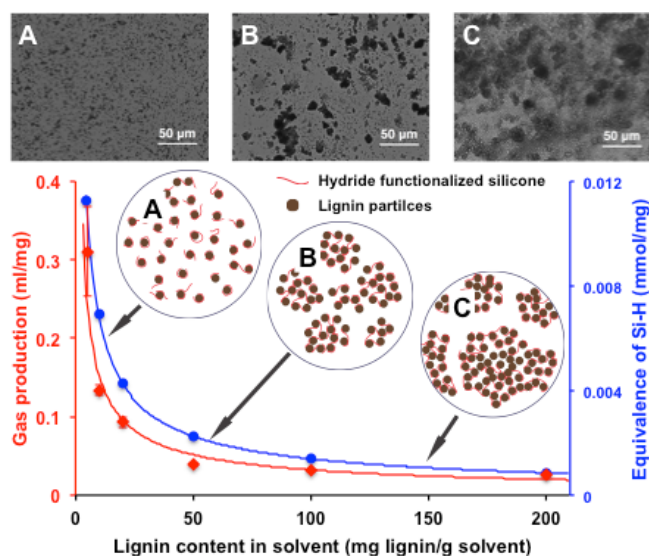


Fig. 1. Gas production (red) and equivalents of hydride used (blue) as a function of lignin content in the solvent. Images A-C are the microscopic images of lignin dispersions at different solid/liquid ratios: A: dispersion of lignin at low content (5 mg/g), evenly distribution of particles; B dispersion of lignin with higher content (50mg/g), formation of clusters; C highly agglomerated lignin particles at concentrated dispersion (200 mg/g).

Lignin particles reacting with HMS-501 or 992 (Table 2) yielded nearly the same volume of gas in spite of their very different SiH concentrations. In the case of HMS-992, the density of functional groups on the silicone backbone may be too high for efficient surface modification. Once initial grafting occurs, the resulting multi-point anchors of a silicone chain block access to reactive groups on lignin. At the other end of the spectrum, DMS-H11 with much lower Si-H density, produced an even lower amount of gas/SiH group. The reason may be attributed to the long polymer chain that, once grafted to the lignin particle surface, protects it from further reaction. PMDS or HMS-301, either with shorter chain length (PMDS) or lower functional density (HMS-301), consumed more reactive lignin surface functional groups.

Each lignin particle can serve as a multifunctional crosslinking point: the surface functional group density is rather high, 0.8-11 μmol mg$^{-1}$ (Fig. 1). Note that not every functional

group on lignin will lead to a productive crosslink. Phenol and methoxyphenyl groups can undergo silylation, potentially leading to crosslinks.[25] However, neither can undergo complete reduction to alkanes: such secondary reduction processes[27] consume SiH groups, but do not lead to crosslinks. For example, the reduction of exposed β-O-4 linkages leads both to lignin backbone cleavage and silylether and reduced methylene groups (Scheme 1).[32] Ideally, the best network would formed at a functionality ratio of 1:1 between SiH:lignin reducible groups (mainly refer to phenol and aryl ethers) provided that this is the only reaction occurring However, this ratio must necessarily vary from 1:1 to 3:1 due to these secondary side reactions that consume Si-H.[41] The optimal formulations for lignin/silicone composites required a co-crosslinker (HMS-301, 501, or 992) in addition to H-PDMS-H spacers (ESI †). Due to the structural complexity of lignin, as well as to facilitate an understanding of the degree to which elastomer properties could be controlled, the SiH:lignin reducible group ratio was tested between 0.5:1 → 4:1.

Table 2. The reactivity of lignin particles and silicone hydride with different chemical structures (lignin content = 50 mg/g).

| | PMDS | DMS-H11 | HMS-301 | HMS-501 | HMS-992 |
|---|---|---|---|---|---|
| Gas production (ml) | 5.83 ±0.39 | 4.89 ±0.32 | 5.63 ±0.16 | 5.10 ±0.29 | 4.96 ±0.22 |
| Average hydride # per -(Si-O)- unit | 0.5 | 0.07 | 0.3 | 0.5 | 1 |
| Chemical structure | H–Si–O–Si– | H–Si–O–(Si–O)$_n$–Si–H   n ≈14 | | | |
| | | | m/n = 3/7 | m/n = 1/1 | n = 0 |
| Mw | 148 | 1000-1100 | 1900-2100 | 900-1200 | 1800-2100 |

Initial examinations of elastomer formulations were confronted with the presence of bubbles in the products. The elimination of defects, including bubbles and voids within an elastomer body, was an important factor in the composite mechanical performance (see below).[38, 39] Depending on the formula, initial structures ranged from porous foams to solid elastomers. Therefore, small amounts of solvent (D$_5$) were added to facilitate egress of bubbles formed during reaction (Table 1). Precursors with higher lignin content required more solvent because not only is the intrinsic viscosity of precursor higher with increased lignin, but the crosslinking density also increases at a rapid rate (Table 1). Adding an antifoam to control bubble nucleation was found to partly reduce the need for solvent to create a bubble free elastomer. As an example, using an antifoam with the formulation containing 41% lignin (LE-41B), the solvent usage could be reduced from ~ 1.5 ml to 1 ml and still obtain a bubble free elastomer. Higher concentrations of lower molecular weight H-PDMS-H could also be used to reduce the incidence of bubbles in elastomers:

in some cases, bubble free elastomers could be made without solvent Table 1, for cross-section images, see ESI †).

The properties of the lignin-filled elastomers were found to vary with lignin content because lignin plays dual roles as both crosslinker and reinforcing agent. A wide variety of lignin contents were examined, ranging from 0.5 to 71wt% in order to control crosslink density, reinforcement and active surface-to-volume ratio of lignin particles. As shown in Fig. 2, the optical property change as a function of lignin concentration is very obvious: additional lignin leads to loss of transparency.

Mechanical properties of the elastomer also varied with lignin content. At lower lignin content, the lignin particles were dispersed unevenly in the elastomer (Fig. 2D). Some of the lignin particles aggregated forming small clusters; moreover, the lignin particles precipitated, forming a bilayered structure (Fig. 3A and D). As a consequence of lower crosslink density and uneven reinforcement (Fig. 2A), the resultant elastomer was very soft and weak (Table 3). However, with an increase in lignin content, the hardness and modulus of elastomer increased while the elongation-at-break decreased (Table 3). These changes could be attributed to the balance of reinforcing and dilution effects. At the optimized lignin content range, as shown in Fig. 2B, the lignin clusters merged together because the volumetric fraction was sufficient (Fig. 3B and E). As one of the best examples, the modulus and elongation-at-break of elastomer were balanced with sample LE-41B, with a lignin content of ~ 41% (Table 3). However, with a further increase of lignin content, the elastomer started cracking even without stress, as shown in Fig. 2G. The amount of silicone was insufficient to hold the particles together (Fig. 2C) and again an uneven distribution of lignin was observed (Fig. 3C and F).
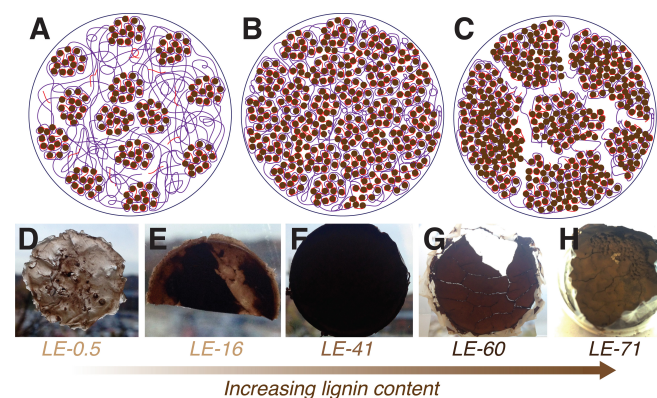


Fig. 2 A schematic illustration of lignin crosslinked silicone networks at different lignin contents. A: low lignin content (0.5 to 16%); B: optimized content range (27 to 57%); and, C: excess content (60 to 71%). Images D-H show the changes in elastomer appearance with different lignin contents.

Mechanical performance also varied with the chemical structure and concentration of the silicone co-crosslinker. The elastomer containing 41% of lignin was used as a model formulation to examine the balance between modulus and elongation-at-break as the molar ratios of hydride to reactive surface functional group on lignin were varied from 0.5:1, 2:1 to 4:1, respectively (LE-41 A/B/C, ESI †). As shown in Table 3,

the modulus (increasing) and elongation-at-break (decreasing) changed significantly with co-crosslinker content. These changes can be attributed to the differences in interfacial cross-linking density between lignin particles and silicone matrix. Low molar ratios of hydride to reactive surface functional groups lead to low crosslinking density and, therefore, poor interfacial control between silicone and lignin. However, as the hydride content was increased (e.g., 2:1 and 4:1), increased reinforcement was observed.[42]
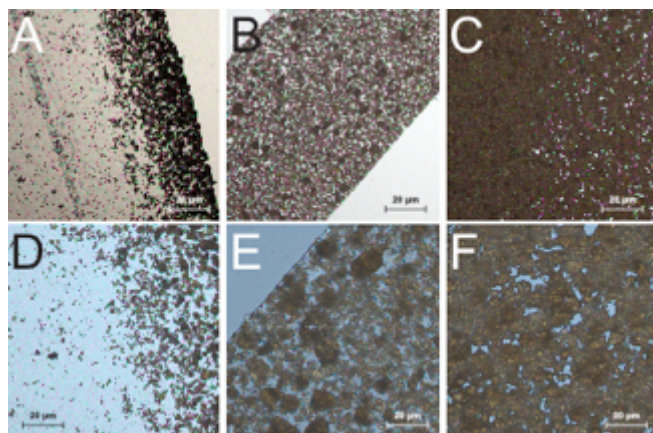


Fig. 3 Cross-sectional images (D-F are the higher magnification images of A-C) of lignin/silicone elastomers of different lignin content: 16% A, D; 41% B,E; 68% C,F, respectively.

Table 3. Mechanical performance of lignin/silicone elastomers, the impact of lignin content, co-crosslinker content, and silicone molecular weight.

| Lignin elastomer # | Shore OO | Shore A | Modulus (MPa) | Elongation-at-break (%) |
|---|---|---|---|---|
| LE-0.5 | 35-45 | -[a] | -[c] | -[c] |
| LE-05 | 40-50 | -[a] | -[c] | -[c] |
| LE-09 | 60-65 | -[a] | -[c] | -[c] |
| LE-16 | 70-75 | -[a] | -[c] | -[c] |
| LE-27 | 85-90 | 30-35 | 0.93 ± 0.22 | 286 ± 40 |
| LE-41A | 85-90 | 35-40 | 1.31 ± 0.02 | 260 ± 14 |
| LE-41B | 85-90 | 45-50 | 3.28 ± 0.39 | 146 ± 17 |
| LE-41C | 85-90 | 55-60 | 5.66 ± 1.01 | 92 ± 21 |
| LE-41D | 85-90 | 65-70 | 5.36 ± 0.73 | 75 ± 15 |
| LE-41E | 85-90 | 65-70 | 4.40 ± 0.14 | 53 ± 5 |
| LE-41F | 85-90 | 45-50 | 1.95 ± 0.49 | 297 ± 30 |
| LE-41G | 70-75 | 20-25 | 0.15 ± 0.01 | 305 ± 21 |
| LE-41H | 85-90 | 55-60[e] | 2.88 ± 0.44 | 71 ± 17 |
| LE-46 | 85-90 | 45-50 | 8.02 ± 1.25 | 83 ± 14 |
| LE-57 | 85-90 | 55-65 | 16.30 ± 2.97 | 35 ± 10 |
| LE-66 | 85-90 | 75-85 | -[d] | -[d] |
| LE-68 | 85-90 | 80-85 | -[d] | -[d] |
| LE-71 | 85-90 | -[b] | -[d] | -[d] |

[a] Hardness could not be measured – the elastomer was too soft. [b] Hardness could not be measured because the foam was cracked under pressure. [c,d] Modulus and elongation-at-break were not measured due to the inferior mechanical properties of the sample or difficulties in making samples with the required dimensions. [e] The hardness test broke the elastomer.

The influence of the silicone chemical structures on elastomer properties was studied by varying the PHMS-PDMS crosslinking silicone ratio, while holding fixed the ratio of hydride to reactive surface functional groups. As shown in Table 3, LE-41G, made using HMS-501 as co-crosslinker, was more elastic due to the spacer siloxane units between the hydride groups; than LE-41H made with HMS-301 as co-crosslinker, which was much more brittle: the elastomer broke during Shore A measurements. Elastomer brittleness resulted from an excess content of low molecular weight HMS-301 in the formulation (more than 50% of silicone was less than 2000 g/mol, Table 1) leading to shorter silicone spacers between crosslinkers.

The molecular weight of H-PDMS-H also affects the mechanical performance of lignin/silicone elastomers. As shown in Table 3, decreasing the silicone chain length resulted in a consistent drop of elongation-at-break and a concomitant rise of the modulus. The entanglement of silicone chains was expected to be an important contribution for elasticity.[43] The elastomer made from higher molecular weight silicone was softer (lower modulus) and tougher (higher elongation-at-break). Note the longer silicone chain will result in a lower crosslinker density (for hydride contents of H-PDMS-H with different Mw, see ESI †). Thus, the mechanical performances of the lignin/silicone elastomers could be easily tuned by changing the SKL content, ratio of crosslinker to co-crosslinker, and molecular weight of H-PDMS-H and co-crosslinker.

The ability to control the final composite structure hinges on the competition between covalent bond formation in the developing network developing and gas production. Therefore, the rates for these two processes need to be manipulated in order to obtain elastomers with desirable structures. In addition to the factors just described, the structure of lignin/silicone elastomers varied with the content of lignin and co-crosslinker (Fig. 4). At low lignin or high co-crosslinker content, undesirable voids in the elastomer could not be avoided even with use of solvent and antifoam (see above). With either an increase of co-crosslinker or decrease of lignin concentration, the network develops too fast for the gas to escape, a problem confounded by the rapid rise of viscosity. Therefore, the content of lignin and co-crosslinker should be in optimized ranges for a defect free elastomer.
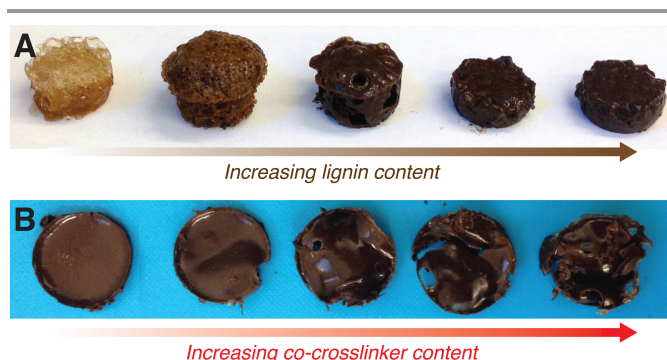


Fig. 4. Structure evolution of silicone foam/elastomer with: A: increasing lignin content, and, B: co-crosslinker content

Silicone elastomers are known for their resistance to a wide temperature range (up to 300 °C) and extreme environments.

How would the presence of lignin affect these thermal properties? The TGA of selected precursor samples were first run to demonstrate the stability of the constituents with increasing temperature. Lignin starts decomposing at 170 °C, while silicone starts to decompose above 350 °C (ESI †). The lignin/silicone elastomer, the composite of both materials, also starts to decompose at 170 °C, and from 170 to 300 °C the decomposition occurred at a constant rate.
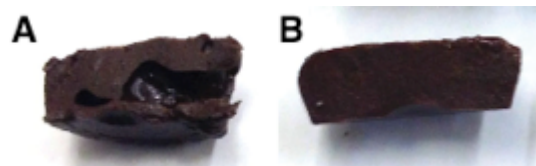


Fig. 5. Elimination of bubble defects by solvent: A no added solvent, B with $D_5$

The mechanical properties of the samples were also tested after aging in air at either 170 and 250 °C. As shown in Table 4, the elastomer demonstrated considerable resistance to high temperature without showing significant change on elongation-at-break. It was initially surprising that the modulus initially dropped with aging at 170 °C, and increased afterwards. However this behaviour has been attributed to the competition between degradation and repolymerization of lignin at this temperature. After the initial few hours, the repolymerization of lignin occurs, leading a more condensed polymer structure with a concomitant increase of the elastomer modulus.[44, 45]

Table 4. The mechanical performance of lignin/silicone elastomers after treatment at higher temperatures and selected organic solvent

| Lignin elastomer # | Condition | Shore OO | Shore A | Modulus (MPa) | Elongation-at-break (%) |
|---|---|---|---|---|---|
| LE-41B | Control | 85-90 | 45-50 | 3.28 ± 0.39 | 146 ± 17 |
| | 170 °C (3 h, air) | 85-95 | 50-55 | 2.02 ± 0.05 | 174 ± 20 |
| | 170 °C (8 h, air) | ~ 95 | 65-75 | 4.09 ± 0.50 | 132 ± 12 |
| | 170 °C (96 h, air) | ~ 95 | 75-80 | 4.92 ± 0.50 | 123 ± 18 |
| | 250 °C (3 h, air) | 90-95 | 55-60 | 3.01 ± 0.07 | 146 ± 20 |
| | Toluene (24 h) | 85-90 | 50-55 | 2.26 ± 0.14 | 172 ± 24 |
| | THF (24 h) | 80-85 | 35-40 | 1.62 ± 0.65 | 198 ± 23 |

The resistance of the composite to ordinary organic solvents was also tested. Due to the combination of hydrophilic (lignin) and hydrophobic (silicone), the lignin-elastomer was found to undergo swelling: <50% in $H_2O$, isopropanol, methanol; <100% in acetone, toluene, dimethyl sulfoxide, and; >150% in tetrahydrofuran (ESI †). Significant weight loss (~ 25%) of the elastomer was only found in the presence of tetrahydrofuran, which is a good solvent for both silicone and lignin. The elastomers extracted in toluene or tetrahydrofuran, respectively, were characterized after extraction. As shown in Table 4, both of the elastomers exhibited deceases in modulus and increasing of elongations-at-break, which might be the result of loss of

organosoluble integration of PDMS and lignin fragments, or lignin fragments.

The properties of the composites described above match those of some low consistency silica-reinforced silicone elastomers, with respect to elongation at break, for example. Higher mechanical properties will result from the use of additional lignin as a reinforcing, but not crosslinking filler and, or smaller lignin particle sizes: both options are currently being examined.

Bio-renewable resources have attracted increasing attention from both the academy and industry. Lignin, as one of the most abundant naturally occurring polymers, is rarely used as a raw material owing to the complexity of lignin structure, and difficulty of processing it. The combination of lignin with silanes using the Piers-Rubinsztajn leads to reinforced silicone elastomers with easily controlled properties that are formed under very mild conditions. Silicone elastomers are widely used in applications ranging from biomedical implants to bathroom sealants. Their properties are unmatched by organic polymers. The utilization of a renewable, recyclable reinforcing agent leads to a new class of silicone elastomers whose properties do not require the user to see 'green' as a compromise; the lignin product compares favorably with its synthetic counterpart.

## Conclusions

The Piers-Rubinsztajn reaction can be used to surface modify softwood lignin particles with silicone groups: the surface density of functional groups was 0.8-11 μmol mg$^{-1}$. In a one step process, under the same conditions, silicone polymers bearing SiH groups could both surface modify the lignin and undergo crosslinking leading to foams and elastomers. The modulus and elongation-at-break of lignin/silicone elastomers could be readily tuned by lignin content and molecular weight of silicones: products were prepared with properties that are comparable to commercial products. The elastomer exhibited excellent resistance to high temperature aging and acceptable resistance to solvent extraction. This work demonstrates that lignin can serve as efficacious green elastomer fillers.

## Notes and references

*Jianfeng Zhang, Yang Chen, Paul Sewell and Michael A. Brook, Chemistry and Chemical Biology, McMaster University, 1280 Main St. W., Hamilton, Ontario, Canada L8S 4M1. Fax: +1-(905) 522-2509; Tel: +1-(905) 525-9140 ext. 23483; E-mail: mabrook@mcmaster.ca.*

† Electronic Supplementary Information (ESI) available: Equipment and chemistry associated with titration of lignin surfaces, IR spectra of silicone-modified lignin surfaces, mathematic calculation for the molar ratio of hydrosilane to reactive functional groups on lignin surface, images of bubble/smooth elastomer made from excess/proper catalyst loading, tables of hydride contents of H-PDMS-H of different Mw, image

of bubble free elastomer LE-41E, solvent resistance tests; and TGA curves for lignin, lignin elastomer, and pure silicone elastomer under air. See DOI: 10.1039/b000000x/

1.  I. A. Pearl, *J. Am. Chem. Soc.*, 1942, **64**, 1429-1431.
2.  M. P. Pandey and C. S. Kim, *Chem. Eng. Tech.*, 2011, **34**, 29-41.
3.  J. Zakzeski, P. C. A. Bruijnincx, A. L. Jongerius and B. M. Weckhuysen, *Chem. Rev.*, 2010, **110**, 3552-3599.
4.  A. Hatakka, in *Biopolymers Online*, Wiley-VCH Verlag GmbH & Co. KGaA, 2005.
5.  N. Yan, C. Zhao, P. J. Dyson, C. Wang, L.-t. Liu and Y. Kou, *ChemSusChem*, 2008, **1**, 626-629.
6.  E. E. Harris, J. D'Ianni and H. Adkins, *J. Am. Chem. Soc.*, 1938, **60**, 1467-1470.
7.  A. Oasmaa, R. Alén and D. Meier, *Bioresource Technology*, 1993, **45**, 189-194.
8.  A. Rahimi, A. Ulbrich, J. J. Coon and S. S. Stahl, *Nature*, 2014, **515**, 249-252.
9.  H. Hisano, R. Nandakumar and Z.-Y. Wang, *In Vitro Cell. Dev. Biol. Plant*, 2009, **45**, 306-313.
10. C. Heitner, D. Dimmel and J. A. Schmidt, *Lignin and Lignans: Advances in Chemistry*, CRC Press, 2010.
11. F. S. Chakar and A. J. Ragauskas, *Ind. Crop. Prod.*, 2004, **20**, 131-141.
12. W. Boerjan, J. Ralph and M. Baucher, *Ann. Rev. Plant Bio.*, 2003, **54**, 519-546.
13. J. Qin, M. Woloctt and J. Zhang, *ACS Sus. Chem. Eng.*, 2013, **2**, 188-193.
14. A. Tejado, C. Peña, J. Labidi, J. M. Echeverria and I. Mondragon, *Bioresour. Technol.*, 2007, **98**, 1655-1663.
15. A. Donmez Cavdar, H. Kalaycioglu and S. Hiziroglu, *J. Mater. Proc. Tech.*, 2008, **202**, 559-563.
16. B. Zhao, G. Chen, Y. Liu, K. Hu and R. Wu, *J. Mater. Sci. Lett.*, 2001, **20**, 859-862.
17. K. Hofmann and W. G. Glasser, *J. Wood Chem. Tech.*, 1993, **13**, 73-95.
18. T. N. M. T. Ismail, H. A. Hassan, S. Hirose, Y. Taguchi, T. Hatakeyama and H. Hatakeyama, *Polym. Int.*, 2010, **59**, 181-186.
19. Y.-L. Chung, J. V. Olsson, R. J. Li, C. W. Frank, R. M. Waymouth, S. L. Billington and E. S. Sattely, *ACS Sus. Chem. Eng.*, 2013, **1**, 1231-1238.
20. M. Thunga, K. Chen, D. Grewell and M. R. Kessler, *Carbon*, 2014, **68**, 159-166.
21. H. Chung and N. R. Washburn, *ACS Appl. Mater. Interfaces*, 2012, **4**, 2840-2846.
22. D. Feldman, M. Lacasse and R. St. J. Manley, *J. Appl. Polym. Sci.*, 1988, **35**, 247-257.
23. C. Ciobanu, M. Ungureanu, L. Ignat, D. Ungureanu and V. I. Popa, *Ind. Crop. Prod.*, 2004, **20**, 231-241.
24. D. S. Argyropoulos, H. Sadeghifar, C. Cui and S. Sen, *ACS Sus. Chem. Eng.*, 2013, **2**, 264-271.
25. D. J. Parks and W. E. Piers, *Journal of the American Chemical Society*, 1996, **118**, 9440-9441.
26. D. J. Parks, J. M. Blackwell and W. E. Piers, *The Journal of Organic Chemistry*, 2000, **65**, 3090-3098.
27. V. Gevorgyan, M. Rubin, S. Benson, J.-X. Liu and Y. Yamamoto, *The Journal of Organic Chemistry*, 2000, **65**, 6179-6186.
28. V. Gevorgyan, M. Rubin, J.-X. Liu and Y. Yamamoto, *The Journal of Organic Chemistry*, 2001, **66**, 1672-1675.
29. J. Cella and S. Rubinsztajn, *Macromolecules*, 2008, **41**, 6965-6971.
30. M. J. Gretton, B. A. Kamino, M. A. Brook and T. P. Bender, *Macromolecules*, 2011, **45**, 723-728.
31. M. Brook, J. Grande and F. ß. Ganachaud, in *Silicon Polymers*, ed. A. M. Muzafarov, Springer Berlin Heidelberg, 2011, vol. 235, pp. 161-183.
32. J. Zhang, Y. Chen and M. A. Brook, *ACS Sus. Chem. Eng.*, 2014, **2**, 1983-1991.
33. E. Feghali and T. Cantat, *Chem. Commun.*, 2014, **50**, 862-865.
34. A. P. Quist, E. Pavlovic and S. Oscarsson, *Anal. Bioanal. Chem.*, 2005, **381**, 591-600.
35. J. W. Zhou, A. V. Ellis and N. H. Voelcker, *Electrophoresis*, 2010, **31**, 2-16.
36. D. R. Paul and J. E. Mark, *Prog. Polym. Sci.*, 2010, **35**, 893-901.
37. E. L. Warrick and P. C. Lauterbur, *Ind. Eng. Chem.*, 1955, **47**, 486-491.
38. A. S. Fawcett, J. B. Grande and M. A. Brook, *J. Polym. Sci., Part A: Polym. Chem.*, 2013, **51**, 644-652.
39. J. B. Grande, A. S. Fawcett, A. J. McLaughlin, F. Gonzaga, T. P. Bender and M. A. Brook, *Polymer*, 2012, **53**, 3135-3142.
40. J. J. Kilbane Ii and S. Le Borgne, in *Studies in Surface Science and Catalysis*, eds. V.-D. Rafael and Q.-R. Rodolfo, Elsevier, 2004, vol. Volume 151, pp. 29-65.
41. C. W. Macosko and J. C. Saam, *Polym. Bull.*, 1987, **18**, 463-471.
42. B. B. Boonstra, *Polymer*, 1979, **20**, 691-704.
43. K. Sivasailam and C. Cohen, *J. Rheology*, 2000, **44**, 897-915.
44. J. Li, G. Henriksson and G. Gellerstedt, *Bioresource Technology*, 2007, **98**, 3061-3068.
45. M. Wayman and M. G. S. Chua, *Can. J. Chem.*, 1979, **57**, 2599-2602.